The 2015 World Congress on
Advances in Civil, Environmental, and Materials Research (ACEM15)
Incheon, Korea, August 25-29, 2015

Dynamic reliability analysis of offshore wind turbine support structure under earthquake

*Gee-Nam Lee[1)], Dong-Hyawn Kim[2)], Yong-Jei Lee[3)]

[1), 2)] *Department of Ocean Science and Engineering, Kunsan National University, Kunsan, 573-701, Korea*
[3)] *Chang Minwoo Structural Consultants, Seoul, 135-907, Korea*
[2)] welcomed@naver.com

ABSTRACT

Seismic reliability analysis of jacket type support structure for offshore wind turbine was performed. When defining the limit state function by using dynamic response of support structure, a number of dynamic calculations should be done in such approach as First Order Reliability Method. That means analysis cost goes too much high. In this paper, a new reliability analysis approach using static response is used. Dynamic effect of the response is considered by introducing a new parameter called Peak Response Factor. The probability distribution of Peak Response Factor can be estimated by using peak value in dynamic response. The probability distribution of Peak Response Factor was obtained for a set of ground motions. Numerical example was presented to compare the proposed approach with conventional static response based approach.

1. INTRODUCTION

On the sea area, there exist the ordinary loads such as wave and wind as well as the occasional loads such as earthquake, typhoon and tsunami. Among them, the seismic load can cause the most severe damage on the structures. Recently, more frequent and bigger earthquakes have been observed on the sea; therefore, the safety evaluation of the offshore structures under earthquake condition is very important. The existing seismic design followed the deterministic analysis method, which would contain the uncertainties in the applied loads and the soil properties. These uncertainties must be considered to prevent non-conservative or conservative design so as to achieve an accurate structural evaluation. Many active studies have been conducted to apply the uncertainties of variables to the design in response to the increasing needs of the reliability design (Bush and Manuel, 2009; Zhang et al., 2010). In the existing reliability analysis, the seismic load was converted into a static load which didn't account for the frequency characteristic so that the calculated probability of failure might not be accurate (Lee and Kim, 2011). The reliability analysis only with the static seismic load is not appropriate and one with the dynamic seismic load must be conducted.

[1)] Graduate Student
[2)] Professor
[3)]

However, the dynamic seismic analysis will take lots of time requiring repetitive structural analysis on the estimation of the response surface and the reliability analysis. By using the peak response factor which is defined as a ratio of dynamic response to static response, the time issue can be solved with dynamic effects(Lee and Kim, 2014).

In this study, the reliability analysis with peak response factor for the dynamic effects was conducted. The seismic load, soil property, and peak response factor were considered as probability variables, and a limit state function was defined by the response surface method. Through the defined limit state function, the reliability analysis with First-Order Reliability Method (FORM) was conducted (Hasofer et al., 1974). The probability variables other than the normal distribution was defined by Rackwitz-Fiessler method for mean and standard deviation (Rackwitz and Fiessler, 1978). A jacket structure used for oil drilling for a long time was used for an example. The reliability analysis results from Level III with peak response factor was assumed true and applied. In this study, the real structure with multi Degree Of Freedom (DOF) was used to verify the peak response factor, while a single degree of freedom model was used in Lee and Kim's study (2014). The conventional Monte Carlo Simulation(MCS) requires lots of trials and many application difficulties are expected. The MCS based Latin Hypercube Sampling(LHS) was used in this study, which requires relatively less trials to produce satisfying results. The FORM was also conducted considering the peak response factor with dynamic properties as a constant to review the effect on the results.

2. Theory

2.1 Reliability analysis

The reliability analysis can be sorted as three levels according to designer's requirements: Sampling method (Level III) that produces lots of random sampling numbers to get the probability of failure in a direct way; Approximate solution (Level II) around the failure point using the defined limit state function; Safety evaluatioin (Level I) in a simple way by applying the factors to the load function and the resistance function. The Level III method can produce a relatively accurate probability of failure but it requires many samples because the probability of failure used to be very low from the engineering point of view.

2.2 Response surface method

To perform the reliability analysis, a limit state function should be defined by the probability variables and the structural response such as deflection and rotation are considered as dependent variables. The limit state function defined by the variables are expressed in the form of implicit function and it makes the analysis difficult. The Response Surface Method (RSM) can approximate the limit state function into the explicit function to make analysis easier (Scheuller et al., 1987). The response surface can be obtained by selecting the sample points in a constant interval from the center, and performing structural analysis from those points. (Khuri and Cornell, 1987). Each sample point can be expressed by Eq. (1).

$$\mathrm{X_i} = \mathrm{X_i^C} \pm \mathrm{h_i}\sigma_{X_i} I_i \tag{1}$$

Where, X_i^C and σ_{X_i} are the mean and standard deviation of variable X_i, respectively, and h_i is the expansion width, I_i is the scattering index.

2.3 Peak response factor

The dynamic peak response and the joint probability density function $f_{R_p,X}$ are expressed by Eq. (2). The damage probability P_f is a volume of the probability density function where the limit state function belongs to negative numbers, and expressed by Eq. (3).

$$f_{R_p,X} = f_{R_p|X}(r_p|x)\, f_X(x) \tag{2}$$

$$P_f = \int_{g<0} f_{R_p,X}(r_p, x) dr_p dx = \int_{-\infty}^{\infty} f_{R_p|X}(r_p|x) f_X(x) dr_p dx \tag{3}$$

In Eq. (2), f_X is a probability density function of each variable, $f_{R_p|X}$ is a probability density function of dynamic peak response to corresponding variables. x and r_p are one variable and a dynamic peak response corresponding to the variable. g in Eq. (3) is a limit state function.

The reliability analysis requires repetitive structural analysis until getting convergent reliability index. In general, a static response is used because getting dynamic peak response every time is not easy. In this study, to apply the existing method considering the dynamic effects, a ratio of dynamic peak response (R_p) to static response (R_{st}) was used as shown in Equation 4. The ratio (R_n) is called a Peak Response Factor (PRF).

$$R_n = R_p / R_{st} \tag{4}$$

From the Eq. (4), under the assumption that the dynamic peak response is proportional to the static response when the dynamic features does not change according to the stochastic variables, the limit state function can be defined by Eq. (5).

$$g(X) = R_{all} - R_n R_{st} \tag{5}$$

Expressing the peak response factor and the joint probability density function of variables, and the limit state function on the normal distribution space, the reliability index (β) which is the shortest distance between the origin and the failure surface can be obtained.

3. Numerical analysis

3.1 Model and environmental condition

A commercial program ANSYS Ver. 12.0 (Ansys Inc, 2009) was used for modeling and numerical analysis. A 5MW offshore wind turbine of NREL(National Renewable Energy Laboratory) reference model(Jonkman et al., 2009) was used. A jacket structure was used to accord with the environmental condition in South west coast in Korea. A beam element was used for tower and jacket, and the Rotor and Nacelle (RNA) was converted into a concentrated mass on each center of gravity by mass element as shown in Figure. 1(a).

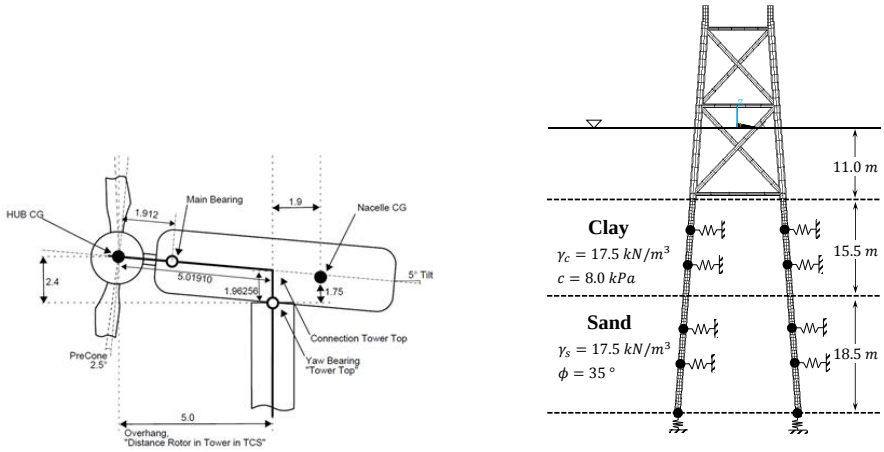

(a) Center of gravity for RNA (b) Finite element model and soil profile

Fig. 1 Offshore Wind Turbine and Soil Profile

3.1.1 Foundation model

As shown in Figure. 1(b), the supports are connected with the foundation composed of cohesive soil and sandy soil, which have a depth of 15.5 m and 18.5 m, respectively. In general, when a load is applied to a structure, a displacement happens along the load direction and also foundation reaction happens to resist the displacement. The relationship between the load and displacement increases non-linearly. To express the nonlinear effect of the foundation, the API RP 2A(American Petroleum Institute, 2007) recommends the *p-y* curve considering the pile diameter and the effective specific weight.

A *p-y* curve for cohesive soil is listed in Table 1, and the ultimate bearing force (p_u) by Eq. (6) is used for *p-y* curve. Where, X, c, D, γ and J are the depth from the surface, undrained shear strength, pile diameter, effective specific weight and experience constant, respectively. X_R is a critical depth calculated by Eq. (7). y_c is a parameter of the critical displacement calculated by Eq. (8). ε_c is a constant strain corresponding to a half of the maximum stress from the undrained compressive test.

Table 1 p-y curves under cyclic loading

$X > X_R$		$X < X_R$	
p/p_u	y/y_u	p/p_u	y/y_u
0.00	0.0	0.00	0.0
0.23	0.1	0.23	0.1
0.33	0.3	0.33	0.3
0.50	1.0	0.50	1.0
0.72	3.0	0.72	3.0
0.72	∞	0.72 X/X_R	15.0
-	-	0.72 X/X_R	∞

$$\mathrm{p_u} = \begin{cases} 3c + \gamma X + J\left(\frac{cX}{D}\right) \\ \\ 9c \quad (for\ X \geq X_R) \end{cases} \tag{6}$$

$$\mathrm{X}_R = \frac{6D}{\frac{\gamma D}{c} + J} \tag{7}$$

$$\mathrm{y_c} = 2.5\varepsilon_c D \tag{8}$$

The *p-y* curve for sandy soil can be calculated by Eq. (9). k, H and A are initial foundation reaction factor, penetration depth of pile and a factor for repetitive load and static load, respectively.

$$p = Ap_u tanh\left[\frac{kHy}{Ap_u}\right] \tag{9}$$

$$A = \begin{cases} 0.9 & (for\ cyclic\ loading) \\ \\ \left(3 - 0.8\frac{H}{D}\right) \geq 0.9 & (for\ static\ loading) \end{cases} \tag{10}$$

The ultimate bearing force can be obtained by Eq. (11) using the minimum of calculated p_{us} and p_{ud}.

$$p_u = \begin{cases} p_{us} = (C_1 H + C_2 D)\gamma H \\ \\ p_{ud} = C_3 D\gamma H \end{cases} \tag{11}$$

Where, the constants C_1, C_2, C_3 for the ultimate bearing strength and the initial foundation reaction factor which is used for *p-y* curve can be estimated using internal friction angle (ϕ') in Figure .2 and 3.

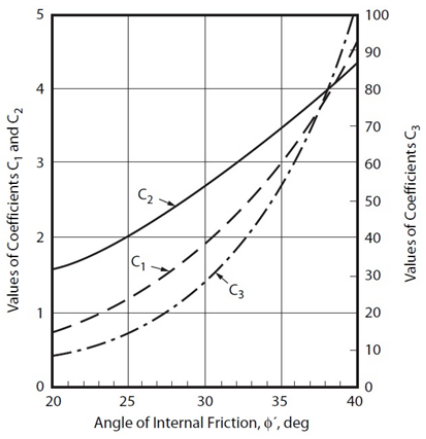

Fig. 2 Coefficients according to phi

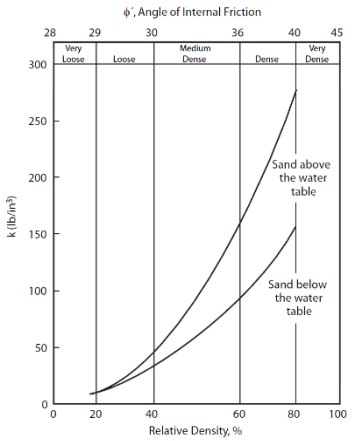

Fig. 3 Initial modulus of subgrade reaction

Figure. 4 shows several relations between the loads and the displacements according to the soil properties in form of the *p-y* curve.

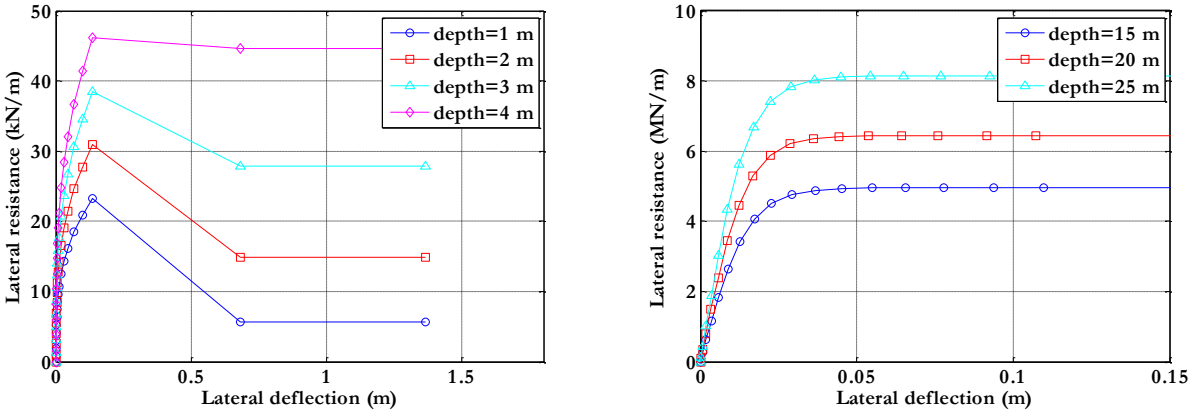

(a) Clay layer (b) Sand layer

Fig. 4 p-y curves for soils

3.1.2 Additional mass

In this study, a additional mass method proposed by Goyal and Chopra (1989) was used because the offshore structures must consider the effect of the sea water. Suppose the sea water was non-compressive fluid, this method consider the water pressure below the sea level of a cylindrical support structure as an equivalent additional mass. The estimated additional mass is regarded as a mass element. Eq. (12) and (13) show how to calculate the additional mass on both outside (m_a^o) and inside (m_a^i) of the structure. Where z, ρ_w, r_o, r_i, H_o and H_i are total length immersed in the water, specific weight of the sea water, outer and inner diameter of the support structure, outer and inner height of the support structure, respectively. a_m is expressed by $(2m-1)\pi/2$. By inserting E_m and D_m in Eq. (14) and (15) into Eq. (12) and (13), the additional mass can be obtained. K_n is a second-type Bessel function with coeeficient of n, and I_n is a first-type Bessel function with coefficient of n.

$$m_a^o = (\rho_w \pi r_o^2)\left\{\frac{16}{\pi^2}\frac{H_o}{r_o}\sum_{m=1}^{\infty}\left[\frac{(-1)^{m-1}}{(2m-1)^2}E_m\left(a_m\frac{r_o}{H_o}\right)cos\left(a_m\frac{z}{H_o}\right)\right]\right\} \quad (12)$$

$$m_a^i = (\rho_w \pi r_i^2)\left\{\frac{16}{\pi^2}\frac{H_i}{r_i}\sum_{m=1}^{\infty}\left[\frac{(-1)^{m-1}}{(2m-1)^2}D_m\left(a_m\frac{r_i}{H_i}\right)cos\left(a_m\frac{z}{H_i}\right)\right]\right\} \quad (13)$$

$$E_m\left(a_m\frac{r_o}{H_o}\right) = \frac{K_1\left(a_m\frac{r_o}{H_o}\right)}{K_0\left(a_m\frac{r_o}{H_o}\right)+K_2\left(a_m\frac{r_o}{H_o}\right)} \quad (14)$$

$$D_m\left(a_m\frac{r_i}{H_i}\right) = \frac{I_1\left(a_m\frac{r_i}{H_i}\right)}{I_0\left(a_m\frac{r_i}{H_i}\right)+I_2\left(a_m\frac{r_i}{H_i}\right)} \quad (15)$$

The additional mass by pressure on outer and inner of the pile and bracing is shown in Figure. 5. The total additional mass of the sea water is listed in Table 2.

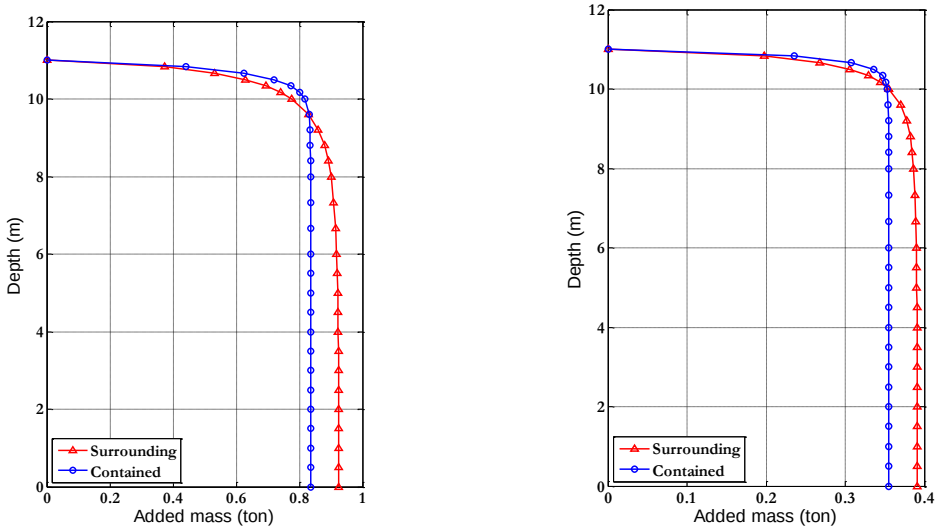

(a) Clay layer (b) Sand layer

Fig. 5 Hydrodynamic added mass on jacket type substructure

Table 2 Added mass according to water depth

water depth (m)	added mass (kg)	
	pile	bracing
11.00	5.64 e-12	3.39 e-12
10.30	1484.52	681.07
8.24	1730.52	739.99
6.18	1752.39	744.21
4.12	1758.10	745.23
2.06	1760.07	745.58
0.00	1760.57	745.67

3.1.3 Seismic load

Before performing reliability analysis, the probability distribution of each variable should be estimated. The seismic intensities per recurrence periods in Korea are proposed in the Korean Port and Harbor Design Standard (MOF, 2005). The HeMOSU-1, which was installed by Korea Electric Power Corporation is under operation for resource investigation and design load computation of South-East offshore wind power complex development. This area is assumed to be a future installation site of the wind power facility for this research. The latitude and longitude by World Geodetic System (WGS84) of the site are 126 ° 07′ 45.30″and 35 ° 27′ 55.17″. Figure. 6 shows the hazard map for the return period of 500 years. From the hazard map, the peak ground

accelerations (PGAs) are estimated and listed in Table 3.

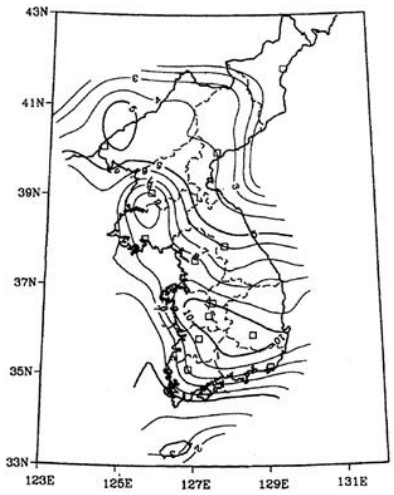

Fig. 6 Seismic hazard (return period – 500 year)

Table 3 Peak ground accelerations at site

average return period(year)	excess probability / period(year)	peak ground acceleration(g)
50	10 % / 5	0.010
100	10 % / 10	0.030
200	10 % / 20	0.045
500	10 % / 50	0.060
1000	10 % / 100	0.080
2400	10 % / 250	0.110
4800	10 % / 500	0.145

The probability distribution of the seismic factor follows the 3-parameter weibull distribution as Eq. (16). It can be estimate by using the scale parameter (σ), shape parameter (k), location parameter (μ) and maximum ground acceleration per average return period. The parameters of the probability distribution can be obtained from the relationship between the return period (T) and seismic factor (K_h^T). F_{K_h} is a cumulative probability distribution of 3-parameter weibull distribution.

$$F_X(x) = 1 - exp\left[\left(\frac{x-c}{b}\right)^k\right] \tag{16}$$

$$K_h^T = F_{K_h}^{-1}(1 - \tfrac{1}{\mathrm{T}}) \tag{17}$$

$$K_h^T = b(\ln(T))^{1/k} \tag{18}$$

The parameters from the regression analysis of Eq. (18) are $\sigma = 4.001 \times 10^{-4}$, $k = 0.3636$, $\mu = 0$. Figure. 7 shows the exceedence probability according to the seismic acceleration from hazard map, and the one from the regression analysis.

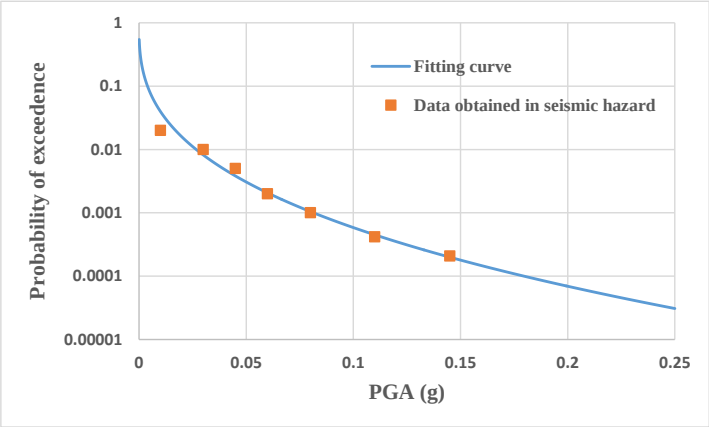

Fig. 7 Estimated probability of exceedance for PGA

The measured seismic time history data is required because a dynamic analysis must be preceded for peak response factor. However, the measured data is not available for the site and a relevant artificial earthquake was produced and used for the research. Abundant data is required to estimate the distribution of the peak response factor; therefore, 50 seeds of each PGA from Table 3 were applied to produce 350 seismic accelerations in total. Figure 8 shows the seismic time history of PGA 0.01g.

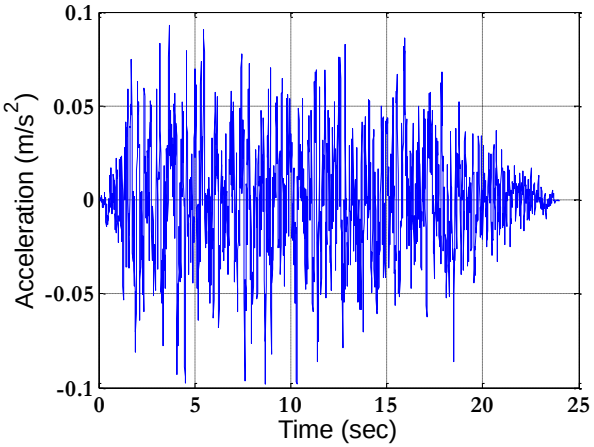

Fig. 8 Time history of seismic acceleration (pga – 0.01g)

3.2 Dynamic amplification

An eigenvalue analysis was performed and the frequency ratio was reviewed to check the dynamic amplification of the structure. The natural frequency and the mass participation ratio of first mode are 0.2645 Hz and 63.52 %, respectively. The forcing frequency differed in the range

between 1.3 and 3.7 according to the seeds. Therefore, the frequency ratio ranged from 5 to 13. As shown in Figure. 9, the dynamic amplification factor corresponding frequency ratio can be less than one.

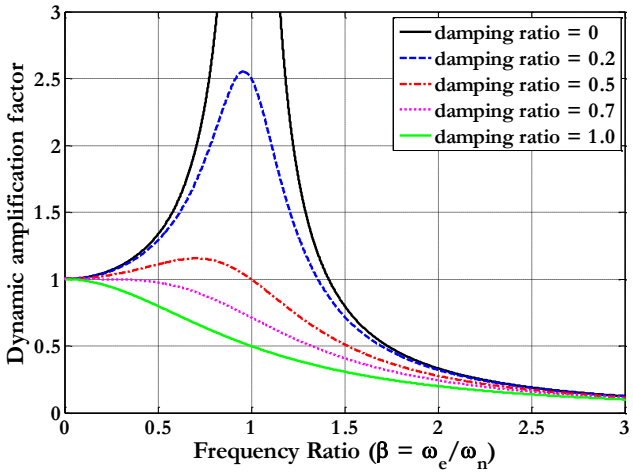

Fig. 9 Dynamic amplification factor (DAF)

3.3 Probability distribution of peak response factor

The distribution of peak response factor can be obtained by dynamic peak response from dynamic analysis and by static response from static analysis. According to the displacement response, the 3-parameter weibull distribution is the most suitable distribution as shown in Figure. 10. the histogram and probability density function of the peak response factor are shown in Figure. 11.

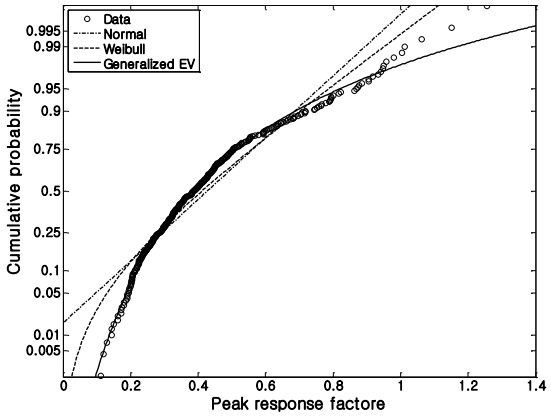

Fig. 10 Probability plot for PRF

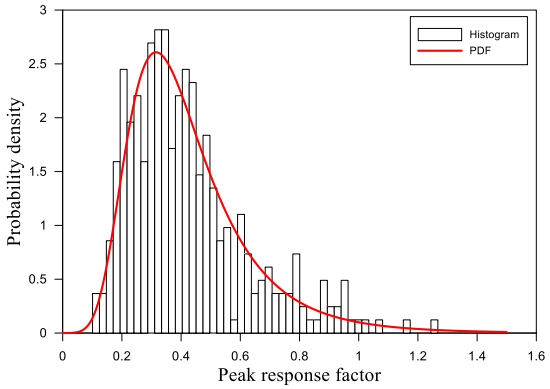

Fig. 11 Histogram and PDF of PRF

As shown in the probability density, the position parameter of x-axis peak response factor is 0.3296. As explained in Figure. 7, when frequency ratio is high, the position parameter of peak response factor can be low. A real earthquake whose main frequencies usually distributes in a low range may produce bigger amplification effect than an artificial earthquake.

3.4 Reliability analysis

The wave load and the wind load must be considered in analysis of an offshore structure. However, during the reliability analysis, the load factors show the Most Probable Failure Point (MPFP) which approaches the ultimate value of probability of distribution through repetitive analysis. For that reason, all wave load, wind load and seismic load are in their ultimate state. In reality, it is hard to happen, so the API RP 2A(2007) recommends to use a seismic load separately from the others. The seismic load and the soil properties are considered as probability variables in the reliability analysis. The distribution of variables and the parameters are listed in Table 4. As mentioned previously, the FORM, Level II reliability analysis method was applied.

Table 4 Characteristics of random variables

random variables	probability distribution	characteristic value
coefficient of earthquake(K_h)	3-parameters weibull	$k = 0.3636, \sigma = 4.001e-4, \mu = 0$
peak response factor(R_n)	3-parameters weibull	$k = 0.1068, \sigma = 0.1419, \mu = 0.3296$
specific weight of clay(γ_{clay})	Log-normal	$\lambda = 2.8511, \xi = 0.1492$
specific weight of sand(γ_{sand})	Log-normal	$\lambda = 2.8792, \xi = 0.1492$
internal friction angle(ϕ')	beta	$q = r = 1.5825$
undrained shear strength(c_u)	Log-normal	$\lambda = 2.0467, \xi = 0.2558$

The inner friction angle of sandy soil can be calculated by the curve fitting using Figure. 2 and 3. In the reliability analysis, if the calculation result is out of range of the inner friction angle, an inappropriate initial foundation reaction factor may be produced. To prevent the erroneous result, the inner friction angle follows the Beta distribution and 30 ° and 40 ° were set as a lower and an upper limit. In the previous researches, the normal distribution was used for soil properties (Yoon et al., 2013; Yoon et al., 2014) but the soil property can not be zero or negative number. If the sensitivity of soil property is very high, the most probable failure point can dramatically low. Considering this kind of possibility, the log normal distribution was used in this study, and the 3-parameter weibull was used for seismic factor and peak response factor. The allowable horizontal displacement (R_{all}) was 25 mm per Korean Road Design Standard.

By using the response surface method, the limit state function was defined as Eq. (19). A sample point for estimation of the response surface was obtained by SD method.

$$g(X) = R_{all} - R_n R_{st}(K_h, \gamma_{clay}, \gamma_{sand}, \phi', c_u) \tag{19}$$

The Level III reliability analysis was performed to verify the result of the Level Ⅱ analysis. In the existing MCS method, 10~100 times of the inverse of the expected damage probability is used as a sample number. This method requires dynamic structural analysis and hard to apply, while LHS requires only small number of samples for damage probability to converge quickly. In this study, the LHS based MCS with dynamic structural analysis was conducted. The numbers in Table 4 same as the Level II analysis condition were applied for probability variables and corresponding characteristics. The peak response factor was not considered as a variable because the dynamic response was used. Total 1,500 times of analysis were performed for sample numbers. Through the curve fitting to the cumulative probability of response, the probability distribution was estimated and the probability of damage was calculated.

3.5 Analysis results

The reliability index of LHS based MCS for verification was 3.3481. After conducting FORM with peak response factor, the reliability index (β) converged on 3.2012 with 4 repetitions showing probability of failure of 6.8428 e-2 %. When the peak response factor was not considered as variable, it was 2.0569 e-1 % with reliability index of 2.8693. The convergence tendency is shown in Figure. 12. In Table 5, the MPFP of each probability variable and the sensitivity factors are listed. In Table 6, the results The results by FORM and the ones by the extraction method are listed.

A 64-bit Windows 7 operating system with 3.4-GHz quad core CPU and 16-GB RAM was used for the analysis. The run-time for the reliability analysis was 6 minutes and 30 seconds, and that for the Level III analysis was 21 days 20 hours and 30 minutes.

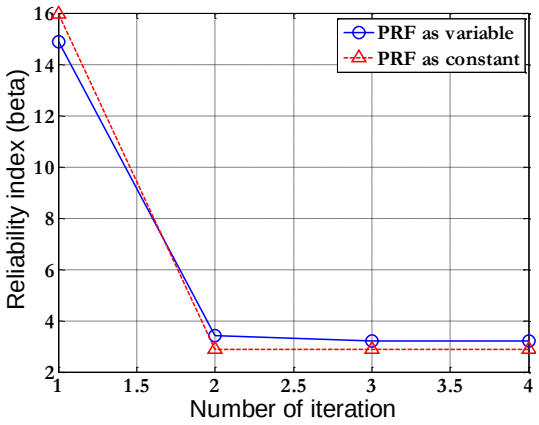

Fig. 12 Convergence of reliability index using FORM

Table 5 MPFPs and sensitivity factors

random variables	case 1 (PRF as variable)		case 2 (PRF as constant)	
	MPFPs	sensitivity factors	MPFPs	sensitivity factors
coefficient of earthquake (K_h)	0.0760 g	- 0.9495	0.0601 g	- 0.9998
Peak response factor (R_n)	0.6046	- 0.3136	-	-
specific weight of clay (γ_{clay})	17.3898 kN/m^3	8.1293 e-3	17.3536 kN/m^3	2.0707 e-2
specific weight of sand (γ_{sand})	17.9126 kN/m^3	3.4023 e-7	17.9126 kN/m^3	6.5059 e-6
internal friction angle (ϕ')	34.9939 °	4.2348 e-4	34.9897 °	1.0674 e-3
undrained shear strength (c_u)	7.7414 kPa	1.8480 e-4	7.7399 kPa	4.6793 e-4

Table 6 Reliability index

	LHS-based MCS	case 1 (PRF as variable)	case 2 (PRF as constant)
Reliability index	3.3481	3.2012	2.8693
Relative error	-	4.3876 %	14.3007 %
Duration time	21일 20시간 30분	6분 30초	3분 10초

4. CONCLUSIONS

The reliability analysis of jacket-type offshore wind turbine support structure was conducted. To consider the dynamic effect in the analysis, a peak response factor (R_n) - the new probability variable

- was used. The response surface was estimated from the horizontal displacement, and using the FRORM, the reliability analysis was conducted by the limit state function. As known from the sensitivity, the seismic factor was the most critical factor and the influence of R_n was also relatively higher than other factors. To verify R_n, the structural analysis was performed by the extraction method. The result showed the reliability index error of 0.1469 compared with the FORM. Although no obvious criteria is available to decide an acceptable error boundary, from the engineering point of view, 4.3876% is thought to be an acceptable error level. That means the reliability analysis using R_n applies the dynamic nature properly. Considering the analysis time, it is not possible to estimate the probability of damage using dynamic structural analysis practically. The Level II, even with some minor error, seems the most suitable method.

The case 1, with R_n, showed higher reliability index than the case 2, without it meaning the probability of damage of the case 1 is low. It can be concluded that this method may produce a conservative design compared with the result of the extraction method. Considering the dynamic character, the more accurate design can be possible: That means the existing static based method does not make proper analysis method.

The structural response can be amplified or reduced according to frequency features. It may cause some safety problem; therefore, the dynamic effect must be reviewed for structural safety evaluation.

Although an offshore structure was studied in this research, the results can be applied to the seismic design of onshore structures because the peak response factor used here is applicable to them. More economical structural design can be possible by estimating the life cycle risk cost through the seismic reliability design.

ACKNOWLEDGEMENT

This work was supported by the New & Renewable Energy of the Korea Institute of Energy Technology Evaluation and Planning (KETEP) grant funded by the Korea government Ministry of Trade, Industry and Energy. (No. 20143010024330, SUCCESS project)

REFERENCES

American Petroleum Institute (API), (2007). “Recommended Practice for Planning, Design and Constructing Fixed Offshore Platforms Working Stress Design.” API Publishing Services.

ANSYS Inc. (2009). ANSYS 12.0 user’s Guide, Canonsburg, PA, USA.

Bush, E. and Manuel, L. (2009). “Foundation Models for Offshore Wind Turbines.” 47th AIAA Aerospace Sciences Meeting Including the New Horizons Forum and Aerospace Exposition, Orlando, Florida, 1-7.

Ministry of Oceans and Fisheries (MOF), (2005). “Engineering Standards Commentaries Port and Harbor Facilities.” Ministry of Oceans and Fisheries, Korea.

Goyal, A., Chopra, A. (1989). “Simplified evaluation of added hydrodynamic mass for intake tower.” Journal of Engineering Mechanics, **115**(7), 1393-1435.

Hasofer, A.M., Line, L.C. (1974). “Exact and Invariant Second Moment Code Format.” Journal of the Engineering Mechanics Division, ASCE, **100**, 111-121.

Jonkman, J., Butterfield, S., Musial, W., Scoot, G. (2009). “Definition of a 5-MW reference wind

turbine for offshore system development." NREL/TP-500-38060.

Khuri, A.I., Cronell, J.A. (1987). "Response Surfaces:Design and analysis." Dekker, New York.

Korea Road Association, (1992). "the Technics of Road Design. the third volume," Korea Expressway Corporation, gim cheon.

Lee, S.G., Kim, D.H. (2011). "Reliability Analysis of Pile Type Quaywall Using Response Surface Method." Journal of Korean Society of Coastal and Ocean Engineers, **23**(6), 407-413.

Lee, S.G., Kim, D.H. (2014). "Reliability Analysis Offshore Wind Turbine Support Structure Under Extreme Ocean Environmental Loads." Journal of Korean Society of Coastal and Ocean Engineers, **26**(1), 33-40.

Rackwitz, R., Fiessler, B. (1978). "Structural Reliability under Combined Random Load Sequences." Computers and Structures, **9**(5), 489-494.

Schueller, G.I., Bucher, C.G., Bourgund, U., Ouypornpasert, W. (1987). "On Efficient Computational Schemes to Calculate Structural Failure Probabilities." Stochastic Structural Mechanics, U.S.-Austria Joint Seminar. 338-410.

Yi, J,H., Kim, S,B., Yoon, G,L., Andersen, L,V. (2015). "Influence of Pile-Soil Interaction on the Dynamic Properties of Offshore Wind Turbines Supported by Jacket Foundations." Proceedings of the 2015 International Ocean and Polar Engineering Conference, 21-26.

Yoon, G.L., Kim, K.J., Kim, H.Y. (2013). "Reliability Analysis of Monopile for a Offshore Wind Turbine Using Response Surface Method." Journal of the Korean Society of Civil Engineers, **33**(6), 2401-2409.

Yoon, G.L., Kim, S.B., Kwon, O.S., Yoo, M.S. (2014), "Partial Safety Factor of Offshore Wind Turbine Pile Foundation in West-South Mainland Sea." Journal of the Korean Society of Civil Engineers, **34**(5), 1489-1504.

Zhang, J., Yugang, L., and Higui, K. (2010). "Application of DSI Techniques to Monopile Foundations of Offshore Wind Turbines Reliability Problems." the Electronic Journal of e-Geotechnical & Geoenvironmental Engineering, **15**, 1-9.